INFLUENCE OF CONNECTION DETAILING IN COLD-FORMED STEEL FRAMES SHEATHED WITH FIBRE-CEMENT BOARDS

INFLUENCE OF CONNECTION DETAILING IN COLD-FORMED STEEL FRAMES SHEATHED WITH FIBRE-CEMENT BOARDS

Nikolas Ringas[1]*, Yuner Huang[1] and Dilum Fernando[1]

[1] Institute for Infrastructure and Environment, School of Engineering, The University of Edinburgh, Edinburgh, United Kingdom
e-mails: n.ringas@ed.ac.uk, yuner.huang@ed.ac.uk, dilum.fernando@ed.ac.uk

Abstract: *Modern construction has been driven by the need of sustainable development, leading to an increased use of modular building elements, such as sheathed cold-formed steel (CFS) panels. Those are utilized as the leading load bearing components in low- to mid-rise buildings given their high strength-to-weight ratio. Recent research has shown that cementitious sheathing boards can substantially increase the stiffness and loading capacity of CFS panels under lateral loads. However, current standards only cover the design of K- or X- bracings to increase the lateral stiffness of CFS panels. Therefore, it becomes critical to quantify the composite action in sheathed cold-formed steel panels induced to the panel by cementitious sheathing boards. As the wall-panel behavior is sequentially affected by the stiffness of individual connectors, it becomes crucial to characterize the connection behavior, given how the most obvious failure modes are expected within the board-fastener interface. This paper presents an experimental investigation on the shear behaviour of connections in CFS systems sheathed with fibre-cement boards employing two different types of fasteners (i.e., with and without wingtips), for a constant diameter of 4.8mm. Recommendations were made with regards to the influence of the fastener type in the ultimate capacity of the connection.*

Keywords: Cold-formed steel; Fibre-cement board; Self-drilling screws; Wingtips; Pushout testing; Cyclic testing

1 INTRODUCTION

Cold-formed steel (CFS) panels are increasingly employed as the main load-bearing component in low- to mid-rise industrial and residential buildings given their advantageous properties, such as high strength-to-weight ratio, offsite manufacturing and reduced overall construction time. Ordinarily, these panels employ CFS strap-bracing in either K- or X-arrangements. However, current construction trends have promoted the use of composite sheathed CFS panels, employing materials such as plasterboard or fiber-cement boards, to provide protection from the elements or for compartmentation purposes. Many studies have provided significant evidence as per the influence of sheathing boards in the in-plane behavior of wall panels. They also proposed that sheathing boards can provide an adequate, or even stronger, substitute for the time-intensive bracing installation [1]–[4]. Nevertheless, composite action of sheathing boards and CFS frames is disregarded in structural design, with the design of only steel-to-steel connections covered [5], [6].

Serrette and Peyton [7] proposed that the ultimate capacity of a wall panel system is a function of the material properties of the sheathing board, the capacity of the steel frame, the ultimate shear capacity of the fastener and the performance of the connection between the steel and the sheathing board. Vieira and Schafer [8] further analysed the stiffness contribution of

the stud-fastener sheathing system, splitting it into three components: rotational, in-plane translational, and out-of-plane translational stiffness. The ultimate strength of the panels will also be affected by its assembly properties, such as screw spacing, stud spacing, wall aspect ratio, and steel and sheathing material thickness [9]–[13].

As all the aforementioned employ fasteners, it becomes inherent to determine the influence of the fastener geometry in the stiffness, ductility and ultimate strength [14]–[16]. Commonly, the connection between the sheathing board and CFS is achieved using self-tapping screws with wings on their tip. However, the wingtips contribute on the enlargement of the screw hole, a construction detail that has been fairly under-investigated in literature. This article presents the experimental characterization of connections employing fiber-cement boards (FCB) and cold-formed steel (CFS), connected using self-tapping screws. The same fastener diameter is employed for fasteners with and without wingtips. Finally, the specimens were tested under a monotonic protocol, in accordance with BS EN 383 [17].

2 EXPERIMENTAL PROGRAMME

The experiments presented herein consist of cold-formed steel (CFS) studs, fiber-cement boards (FCB) and self-tapping screws. The CFS studs are made of S350GD+ZA steel, for a commonly used lipped channel geometry with a 100mm web, 45mm flanges and 10mm lips. The sheathing boards were made of fiber-cement boards with a 12mm thickness, attached to the stud using self-tapping screws with a diameter of 4.8mm, with and without wingtips. The material properties of CFS and FCB were investigated through mechanical testing, while the screws' mechanical and geometrical properties, made of hardened carbon steel, were provided by the manufacturer. Ultimately, the racking behavior of the connection for the composite system was recorded through push-out testing under a monotonic protocol.

2.1 Material testing

2.1.1 Cold-formed steel

Coupon testing was executed to determine the material properties of S350GD+ZA cold-formed steel, for specimens extracted from 500mm long CFS studs in longitudinal direction. The dimensions of the coupons conformed to ISO 6892-1:2019 [18], for a total of three coupons. A 37% purity hydrochloric-acid solution was applied on the gauge length to remove the zinc and aluminum coating, and to allow for the recording of the virgin steel properties.

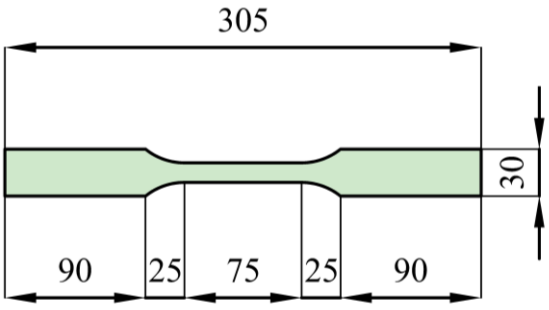

Figure 1: Cold-formed steel coupon geometry (unit – millimeters)

Testing was performed using a 100kN Instron 68FM-100 electromechanical universal testing machine (UTM), with strains measured using a 50mm knife-edged extensometer. The

loading protocol was derived from [19] and applied under displacement control. A loading rate of 0.20mm/min was employed up to the yield plateau, doubled to 0.40mm/min in the hardening region and near to the ultimate strength, and subsequently to 0.80mm/min until fracture. Constant straining was applied for a period of 3 minutes in the yield plateau and pre-ultimate strength range to measure the magnitude of stress relaxation and determine the corresponding rate-independent stress-strain curve for the steel material. The raw data extracted from the actuator controller were presented as measured stress and strain, while the offset curve based on the magnitude of stress relaxation is presented as static stress and strain.

2.1.2 Fibre-cement board

The mechanical properties of fibre-cement board were recorded both in tension and compression, as the material is assumed to exhibit orthotropic behaviour. Three tensile coupons were extracted from the longitudinal direction of a fibre-cement board and cut in compliance with the geometry presented in [15], as illustrated through Figure 2a.

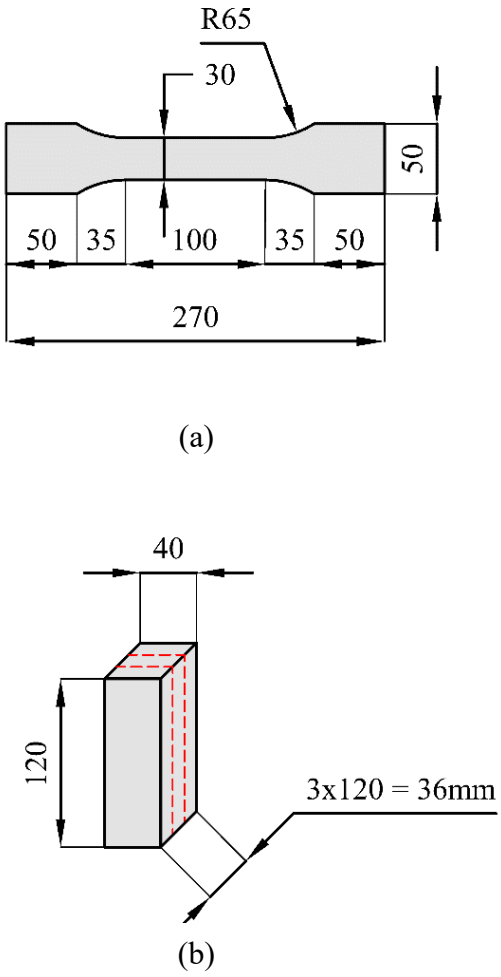

Figure 2: Fibre-cement board materials testing - (a) tensile coupon geometry, (b) compressive coupon geometry (unit – millimeters)

Similarly, a series of three compressive coupons were extracted to obtain the compressive strength parallel to the faces of the board. The compressive coupon specimens consisted of three 12mm plies, with 120mm height and 300mm width, and glued together using a two-component epoxy adhesive. Those were cut into 40mm wide specimens, as illustrated through Figure 2b. Subsequently, they were wrapped with four layers of 15mm-wide unidirectional (UD) carbon-

fibre reinforced polymer (CFRP) ribbon tape at each end, to ensure that no bearing failure is caused by the compressive platens onto the coupons, as presented in Figure 3. The strains were recorded using two strain gauges, one on each side, for the compressive coupons, and the same knife-edged extensometer mentioned in section 2.1.1 for the tensile coupons. Both tests were executed at a constant rate of 0.10mm/min until failure, based on BS EN 383 [17], under displacement control.

Figure 3: Fibre-cement compressive coupon, wrapped with UD CFRP ribbon

2.1.3 Self-tapping screws

As the mechanical properties of commercially available self-tapping screws used in CFS construction are not expected to vary significantly in terms of shear and tensile strength to what is reported from the manufacturer, no further mechanical testing was performed. The push-out tests discussed in Section 2.2 focused on the influence of the wingtips and screw diameter on the ultimate capacity of composite CFS-FCB connections. The purpose of the wingtips is to ensure that the threads do not directly engage with the cement boards and to avoid burn-out of the self-drilling tip before it reaches the steel substrate. However, the wingtip will also cause substantial drill hole enlargement, whose effect on the stiffness of the connection has not been explored. Hence, two types of screws were examined, with and without wingtips, for the same diameter of 4.8mm

Table 1: Geometrical properties for 4.8mm fasteners, with and without wingtip

	4.8mm with wingtip	4.8mm without wingtip
d_s (mm)	3.6	3.6
d_h (mm)	9.5	9.5
p (mm)	1.6	1.8
h_t (mm)	0.6	0.6
L_h (mm)	3.0	3.0
L_t (mm)	23.5	28.0
L_w (mm)	3.5	N/A
L_{tot} (mm)	38.0	38.0

where, d_s is the shank diameter, d_h is the screw head diameter, p is the pitch, h_t is the height of the thread, L_h is the length of the head, L_t is the threaded part length, L_w is the length of the wingtip and L_{tot} is the total length of the fastener.

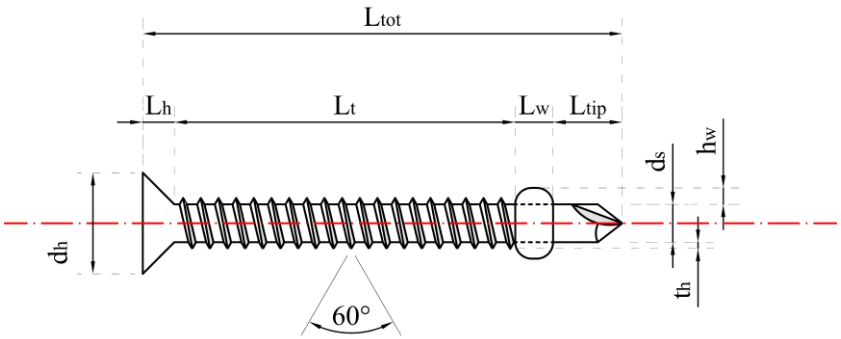

Figure 4: Indicative sketch for the fastener geometry (unit – millimeters)

2.2 Push-out testing

Many push-out testing arrangements have been proposed and modified based on the standard practice for the characterization of the force-slip behavior for embedded steel studs in concrete slabs [20]. The tests conducted herein employed a 230mm single steel stud, as presented in [21]. Two 200mm FCB square boards, one on each side, were fastened to the flanges of the stud with screws at 100mm spacings. The screws were hand-tightened before the screwhead reached the board to avoid overdriving and pre-tensioning the fastener, which would result in recording a higher stiffness while decreasing the capacity and ductility of the connection [8].

Three separate experiments were conducted for each different type of screws discussed in Section 2.1.3, for a total of 6 tests. All the tests were executed using the same UTM employed for the materials testing. The monotonic loading protocol employed was based on [17], [22] and applied through displacement control, as presented in Figure 5. Initially, the specimens were subjected to an initial loading cycle up to 10% of the expected ultimate load (F_u). Subsequently, the specimen was loaded to 40% of its expected ultimate strength and reversed again to 10% at a constant displacement rate of 0.8mm/min. Finally, the specimens were tested to failure at a rate of 1.6mm/min. Load holds were kept at each of the 10% and 40% loading steps, for a period of 30 seconds each.

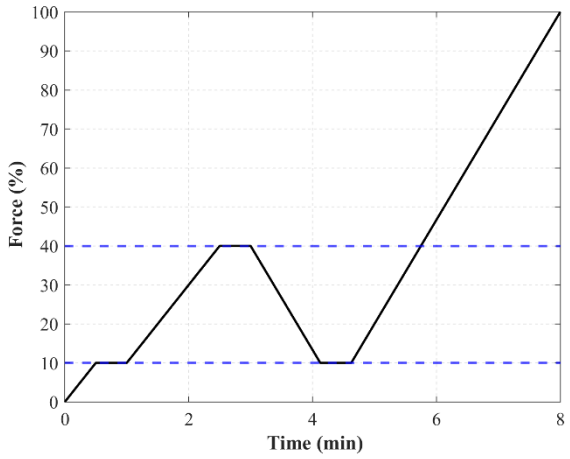

Figure 5: Push-out test protocol

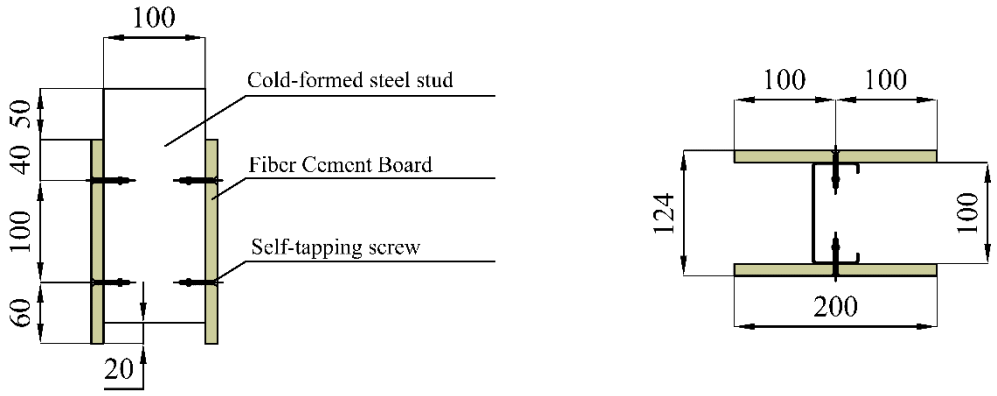

(a) (b)

Figure 6: Push-out test specimen dimensions - (a) side view, (b) top view

3 RESULTS

3.1 Materials testing

The measured and static stress-strain response of cold-formed steel obtained through steel coupon testing is illustrated through Figure 7, with key static mechanical properties such as Young's Modulus (E), yield stress at 0.2% strain offset (f_y), tensile strength (f_u), and strain at fracture (ε_f) presented in Table 2. The labelling system followed starts with the acronym for the material (CFS), followed by its thickness (1p2 = 1.2 mm). The average modulus of elasticity recorded was 193.5 GPa, with an average yield stress of 395.2 MPa and a tensile strength of 500.1 MPa, with the average elongation at fracture being equal to 22.5%.

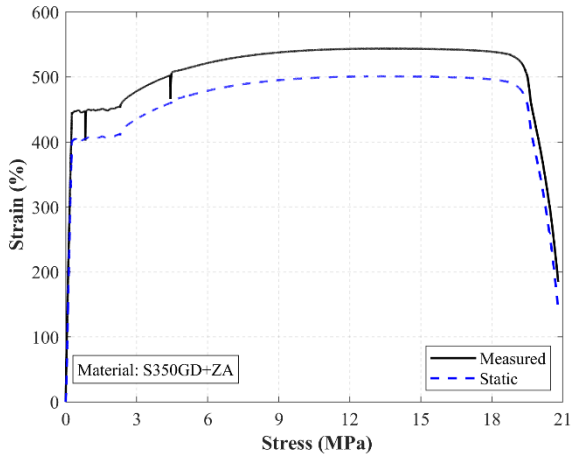

Figure 7: Cold-formed steel - indicative stress/strain response for specimen CFS-1p2_1

Table 2: Cold-formed steel tensile coupon testing

ID	E (GPa)	f_y (MPa)	f_u (MPa)	ε_f (%)
CFS-1p2_1	194.3	404.4	501.0	20.8
CFS-1p2_2	191.2	393.9	504.0	22.0
CFS-1p2_3	195.0	387.2	495.2	24.6
Average	193.5	395.2	500.1	22.5
CoV	0.01	0.02	0.01	0.09

Key averaged material properties for the behavior of fibre-cement boards under tension and compression are presented through Table 3 and Table 4 respectively. A figure combining the

material's stress-strain response under tension and compression is illustrated in Figure 8, with the compressive strength presented on the positive quadrant. Both types of tests recorded an average Young's Modulus around 9 GPa for tension and compression, as illustrated by the dashed line on Figure 8. The material's ultimate compressive strength recorded an average value of 26 MPa which is almost four times larger than its tensile strength.

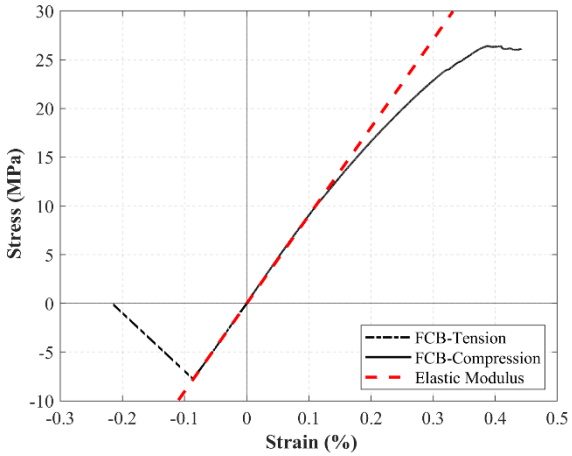

Figure 8: Fibre-cement board material behavior

Table 3: Fibre-cement board tensile coupon testing

ID	E (MPa)	f_u (MPa)	ε_u (%)
FCB-Tens_1	9277.0	7.1	0.076
FCB-Tens_2	8996.4	7.8	0.087
FCB-Tens_3	8890.0	6.2	0.071
Average	9054.5	7.0	0.078
CoV	0.02	0.11	0.10

Table 4: Fibre-cement board compressive coupon testing

ID	E (MPa)	f_u (MPa)	ε_u (%)
FCB-Comp_1	9079.9	26.0	0.36
FCB-Comp_2	8863.3	25.5	0.37
FCB-Comp_3	9025.0	26.4	0.38
Average	8989.4	26.0	0.37
CoV	0.01	0.02	0.03

3.2 Push-out testing

The stiffness per fastener is calculated as the tangent to the force-displacement curve in the 10% to 40% load range and before the load reversals. That is given through the equation provided form [17].

$$K = \frac{F_{40} - F_{10}}{d_{40} - d_{40}}$$

with F and d corresponding to load and slip at the 10% and 40% load reversals. Additionally, the connection ductility is presented as the ratio between the displacement at 80% force after the ultimate connection capacity is reached over the displacement at the 40% load reversal.

$$D = \frac{d_{80u}}{d_{40}}$$

with d_{80u} and d_{40} corresponding to the displacements at the 20% load reduction past the ultimate strength and the displacement at 40% of the ultimate capacity. The force-slip curves for the 4.8 mm fasteners with wingtip and the 4.8 mm fasteners without wingtip are illustrated in Figure 9a and 9b.

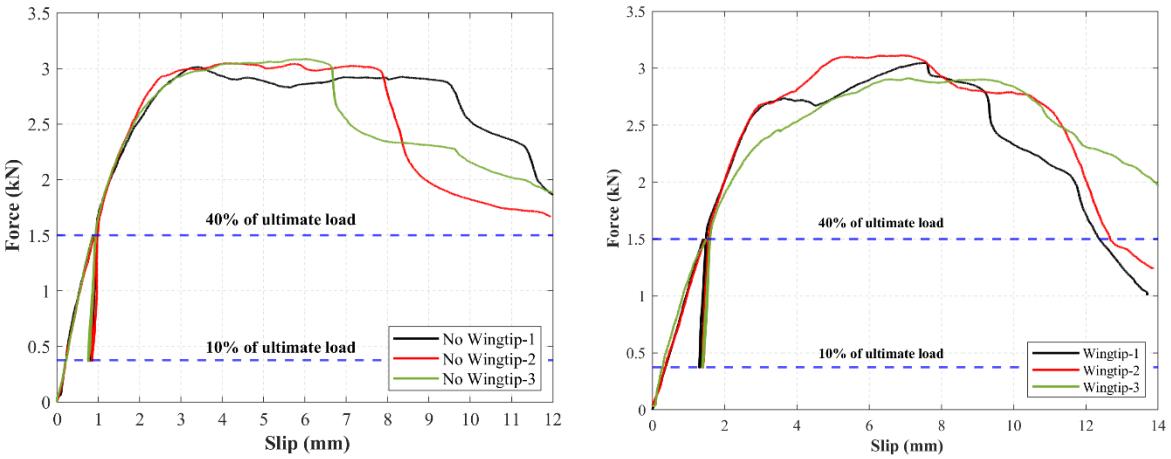

(a) (b)

Figure 9: Push-out test force-slip curves - (a) specimens without wingtip, (b) specimens with wingtip

The sequence of failure initiation deferred between the two types of specimens, although the failure mode looked identical past the ultimate capacity. For the specimens with wingtip fasteners, failure mode initiation occurred due to tilting of the screw until it reached the board interface, given the fact that there is hole enlargement on the sheathing board caused by the wingtip. That was followed by a localized bearing failure to the sheathing board with board cracking in the radial direction, and a subsequent pull-through of the screwhead under excessive displacement. On the contrary, for the fasteners without wingtip, failure was initiated by bearing of the screw shank onto the board, followed by tilting near ultimate capacity and pull-through at high displacement. No local buckling was observed on the inside of the flange of the CFS channel around the screw hole, while the fasteners did not experience any plastic deformations. However, through a macroscopic observation, as presented in Figure 10b, it can be observed that the threads did not engage with the steel plate anymore, possibly attributed to the pitch of the fasteners being larger than the steel thickness.

(a) (b)

Figure 10: Failure modes - (a) bearing failure and cracking on the board, (b) fastener tilting on the inside of the CFS channel for a wingtip specimen

A summary of results for specimens with both types of fasteners, including ultimate force per fastener (F_u), displacement at ultimate load (d_u), connection stiffness (K), ductility (D) and failure mode, are presented through Table 5 and Table 6. There was no substantial increase observed in the ultimate capacity of the connection under the same loading conditions, with both types sustaining a load of 3 kN. However, the ductility of the connection was inversely proportional to the increase in stiffness, which rose by 66% for the specimens without wingtips, as indicated through Figure 11. Finally, the displacement at ultimate strength varied significantly for the wingtip-less specimens, while the winged fasteners experienced a 7.2mm slip on average.

Table 5: Push out testing for 4.8mm fasteners with wingtip

ID	F (kN)	d_u (mm)	K (N/mm)	D (-)	Failure Mode
Wingtip - 1	3.0	7.5	1090.7	6.8	T+B+PT
Wingtip - 2	3.1	6.9	1017.0	7.6	T+B+PT
Wingtip - 3	2.9	7.1	920.2	7.9	T+B+PT
Average	3.0	7.2	1009.3	7.5	-
CoV	0.03	0.04	0.08	0.08	-
T= screw tilting, B = bearing, PT = pull-through					

Table 6: Push out testing for 4.8mm fasteners without wingtip

ID	F (kN)	d_u (mm)	K (N/mm)	D (-)	Failure Mode
No Wingtip - 1	3.0	3.7	1716.0	12.1	B+T+PT
No Wingtip - 2	3.0	4.2	1600.1	9.1	B+T+PT
No Wingtip - 3	3.1	6.0	1716.3	8.3	B+T+PT
Average	3.0	4.6	1677.5	9.8	-
CoV	0.02	0.26	0.04	0.20	-
T= screw tilting, B = bearing, PT = pull-through					

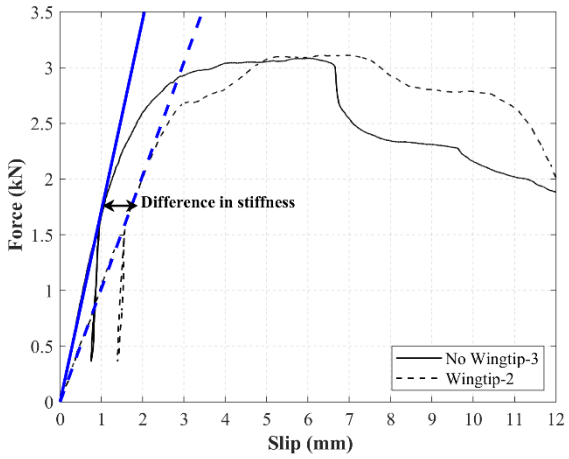

Figure 11: Difference on the stiffness of the connection for specimens with and without wingtips

4 CONCLUSION

An extensive experimental program was carried out to record the racking behavior of connections employed on cold-formed steel frames sheathed with fiber-cement boards, for fasteners with and without wingtips. Materials testing was performed for both CFS and FCB, under tension and compression, to measure the mechanical behavior of the materials employed on sheathed framing systems. Those were followed by single stud push-out tests under a monotonic protocol, to record the force-slip behavior of the connections.

The measured capacity of individual connections remained unaltered, for the two different fastener types. However, through the push-out tests, it was determined that the stiffness of wingtip-less connections is significantly increased, compared to wingtip fasteners. Moreover, the displacement at ultimate force for the wingtip-less connections varied significantly and recorded a lower average value to that of the wingtip connections.

Following the work presented in this study, further investigation will be performed to study connection behavior for different fastener diameters, with and without wings, using various other sheathing materials, such as calcium silicate boards (CSB) and oriented strand boards (OSB/3). The results will be employed as the basis for design specification in composite connections, comprising of sheathing boards and cold-formed steel. Furthermore, they will be employed in an advanced numerical parametric study, addressing the influence of composite action on the lateral behavior of full wall panel assemblies, with potential construction applications and material-efficient structural design.

5 ACKNOWLEDGEMENTS

The authors would like to thank Mr Richard Webb of Newton Steel Framing and Mr Ryan Murphy of Evolution Fasteners for providing the materials necessary to complete the presented experimental work. Finally, the authors would like to thank Mr Mark Partington, Mr Jim Hutchinson and Mr Ralph Cook of The University of Edinburgh, School of Engineering for their assistance in specimen preparation and testing.

REFERENCES

[1] R. M. Lawson, A. Kermani, M. Stergiopoulos, G. Coste, and A. Way, “Diaphragm action in light steel framing by sheathing boards,” Eng Struct, vol. 220, Oct. 2020, doi: 10.1016/j.engstruct.2020.110952.

[2] V. Macillo, L. Fiorino, and R. Landolfo, “Seismic response of CFS shear walls sheathed with nailed gypsum panels: Experimental tests,” Thin-Walled Structures, vol. 120, no. August, pp. 161–171, 2017, doi: 10.1016/j.tws.2017.08.022.

[3] C. L. Pan and M. Y. Shan, “Monotonic shear tests of cold-formed steel wall frames with sheathing,” Thin-Walled Structures, vol. 49, no. 2, pp. 363–370, 2011, doi: 10.1016/j.tws.2010.10.004.

[4] S. H. Lin, C. L. Pan, and W. T. Hsu, “Monotonic and cyclic loading tests for cold-formed steel wall frames sheathed with calcium silicate board,” Thin-Walled Structures, vol. 74, pp. 49–58, 2014, doi: 10.1016/j.tws.2013.09.011.

[5] AISI, “S200-12. North American Standard for Cold-Formed Steel Framing – General Provisions,” American Iron and Steel Institute, p. 49, 2012.

[6] B.S.I., BS EN 1993-1-1:2005+A1:2014 - Eurocode 3. Design of steel structures. General rules and rules for buildings. British Standards Institution, 2005.

[7] R. Serrette and D. Peyton, “Strength of Screw Connections in Cold-Formed Steel Construction,” Journal of Structural Engineering, vol. 135, no. 8, pp. 951–958, Aug. 2009, doi: 10.1061/(ASCE)0733-9445(2009)135:8(951).

[8] L. C. M. Vieira and B. W. Schafer, “Lateral stiffness and strength of sheathing braced cold-formed steel stud walls,” Eng Struct, vol. 37, pp. 205–213, Apr. 2012, doi: 10.1016/j.engstruct.2011.12.029.

[9] S. R. Ayatollahi, N. Usefi, H. Ronagh, M. Izadinia, and M. R. Javaheri, “Performance of gypsum sheathed CFS panels under combined lateral and gravity loading,” J Constr Steel Res, vol. 170, Jul. 2020, doi: 10.1016/j.jcsr.2020.106125.

[10] R. qiang Feng, B. Zhu, P. H. Xu, and Y. Qiu, "Seismic performance of cold-formed steel framed shear walls with steel sheathing and gypsum board," Thin-Walled Structures, vol. 143, Oct. 2019, doi: 10.1016/j.tws.2019.106238.

[11] M. Nithyadharan and V. Kalyanaraman, "Experimental study of screw connections in CFS-calcium silicate board wall panels," Thin-Walled Structures, vol. 49, no. 6, pp. 724–731, Jun. 2011, doi: 10.1016/j.tws.2011.01.004.

[12] A. R. Badr, H. H. Elanwar, and S. A. Mourad, "Numerical and experimental investigation on cold-formed walls sheathed by fiber cement board," J Constr Steel Res, vol. 158, pp. 366–380, Jul. 2019, doi: 10.1016/j.jcsr.2019.04.004.

[13] J. Ye, X. Wang, and M. Zhao, "Experimental study on shear behavior of screw connections in CFS sheathing," J Constr Steel Res, vol. 121, pp. 1–12, 2016, doi: 10.1016/j.jcsr.2015.12.027.

[14] L. Fiorino, T. Pali, B. Bucciero, V. Macillo, M. Teresa Terracciano, and R. Landolfo, "Experimental study on screwed connections for sheathed CFS structures with gypsum or cement based panels," Thin-Walled Structures, vol. 116, pp. 234–249, Jul. 2017, doi: 10.1016/j.tws.2017.03.031.

[15] C. Kyprianou, P. Kyvelou, L. Gardner, and D. A. Nethercot, "Characterisation of material and connection behaviour in sheathed cold-formed steel wall systems – Part 1: Experimentation and data compilation," Structures, vol. 30, pp. 1161–1183, Apr. 2021, doi: 10.1016/j.istruc.2020.12.056.

[16] S. Swensen, G. G. Deierlein, and E. Miranda, "Behavior of Screw and Adhesive Connections to Gypsum Wallboard in Wood and Cold-Formed Steel-Framed Wallettes," Journal of Structural Engineering, vol. 142, no. 4, Apr. 2016, doi: 10.1061/(asce)st.1943-541x.0001307.

[17] British Standards Institution, "BS EN 383:2007 - Timber Structures-Test methods, Determination of embedment strength and foundation values for dowel type fasteners," BSI, 2007.

[18] British Standards Institution BSI, BS EN ISO 6892-1:2019 - Metallic materials - Tensile testing. British Standards Institution BSI, 2019.

[19] Y. Huang and B. Young, "The art of coupon tests," J Constr Steel Res, vol. 96, pp. 159–175, 2014, doi: 10.1016/j.jcsr.2014.01.010.

[20] British Standards Institution, "Eurocode 4 : design of composite steel and concrete structures. Part 1-1: General rules and rules for buildings.," BSI, 2009.

[21] N. Ringas, Y. Huang, and J. Becque, "Fastener behaviour in sheathed light-gauge steel stud walls under cyclic and monotonic actions," 2021, doi: 10.1002/cepa.

[22] American Society for Testing and Materials, "ASTM E2126-19: Standard Test Methods for Cyclic (Reversed) Load Test for Shear Resistance of Vertical Elements of the Lateral Force Resisting Systems for Buildings," 2019.